Acta Neuropathol (2004) 108: 435–442
DOI 10.1007/s00401-004-0907-2

REGULAR PAPER

**Kyoko Noda-Saita · Kazuhiro Terai · Akihiko Iwai
Mina Tsukamoto · Yoshitsugu Shitaka
Shigeki Kawabata · Masamichi Okada
Tokio Yamaguchi**

Exclusive association and simultaneous appearance of congophilic plaques and AT8-positive dystrophic neurites in Tg2576 mice suggest a mechanism of senile plaque formation and progression of neuritic dystrophy in Alzheimer's disease

Received: 11 March 2004 / Revised: 25 June 2004 / Accepted: 28 June 2004 / Published online: 14 September 2004

Abstracts Progression of neuritic dystrophy is a histological hallmark of Alzheimer's disease (AD) in addition to amyloid deposition and neurofibrillary tangle formation. Dystrophic neurites (DNs) are abnormal neurites, and are closely associated with amyloid deposits. To clarify the process of DN formation, we immunohistochemically investigated phosphorylated tau (AT8 and Ser396)-positive DNs and plaques in Tg2576 mice overexpressing human β-amyloid precursor protein (APP) with the Swedish type mutation (K670N/M671L). AT8-positive DNs were exclusively associated with the Congo red-positive plaques examined, and all Aβ_{1-40}-positive plaques appeared to be associated with AT8-positive DNs, whereas there were no AT8-positive DNs with Aβ_{1-42}-positive/Aβ_{1-40}-negative plaques. Since we have previously shown that Aβ_{1-42}-positive plaque precede Aβ_{1-40} deposition, the appearance of congophilic structures is also late. Quantitative analyses were performed on AT8-positive DNs that were associated with congophilic plaques in the cerebral cortex and hippocampus (more than 1,000 plaques). The number of congophilic plaques increased dramatically with age. The area of DNs in the cerebral cortex and hippocampus increased 120- and 60-fold from 11–13 to 20.5 months of age, respectively. Interestingly, the mean ratio of DN area to congophilic plaque area in every plaque was unchanged, approximately 10%, through the ages examined. The mean plaque size was stable with age in both the cortex and hippocampus. These data suggest that the formation of AT8-positive DNs is simultaneous with Congo red-positive plaque development, and that the event may be closely related in the pathological progression of AD.

Keywords Alzheimer's disease · Dystrophic neurite · Congophilic plaque · Tau · Quantitative analysis

K. Noda-Saita (✉) · K. Terai · A. Iwai · M. Tsukamoto
Y. Shitaka · M. Okada · T. Yamaguchi
Neuroscience Research,
Yamanouchi Pharmaceutical Company Limited,
21 Miyukigaoka, Tsukuba,
305-8585 Ibaraki, Japan
E-mail: nodak@yamanouchi.co.jp
Tel.: +81-29-8636519
Fax: +81-29-8562515

S. Kawabata
Molecular Medicine Research,
Yamanouchi Pharmaceutical Company Limited,
21 Miyukigaoka, Tsukuba,
305-8585 Ibaraki, Japan

Introduction

The major pathological features observed in the brain of patients affected by Alzheimer's disease (AD) are the presence of intracerebral and cerebrovascular amyloid deposits, neurofibrillary tangles (NFTs), and loss of subsets of neurons throughout the neocortical, limbic and subcortical areas. Amyloid deposits at the core of senile plaques and on vessel walls have been regarded as one of the most important pathological changes in AD. Senile plaques are classified as diffuse, immature (primitive) or mature (dense-cored and compact) [1, 2, 15]. The major protein component of amyloid is β-amyloid (Aβ), which is 4-kDa peptide of 39–43 amino acids derived from a larger transmembrane amyloid precursor protein (APP) [8, 31]. Mature, congophilic plaques consist of Aβ_{1-40} and Aβ_{1-42}, while diffuse plaques are mostly Aβ_{1-42} [11, 17, 19].

Abnormal neuronal processes known as dystrophic neurites (DNs) have been considered to be another

component of senile plaques or aberrant structures closely associated with intracerebral amyloid deposits (neuritic plaques) of AD patients. DNs are embedded in the edge of amyloid plaque, as are reactive astrocytes and microglia [7, 10]. Neuritic plaques, which contain DNs, have been reported to show a pathological correlation with AD dementia scores [22, 26, 30]. Plaque-associated DNs in non-AD cases were immunolabeled mainly for neurofilament proteins and its phosphorylated form, but only a little for phosphorylated tau proteins, while DNs in severe AD cases were preferentially positive for phosphorylated forms of tau [35]. These reports indicate that DNs positive for phosphorylated tau are very important pathological features closely related to synaptic deficits.

Transgenic mice of the Tg2576 line, which express human βAPP with the Swedish mutation (βAPP695swe, K670N/M/671L), have been established [14], and evidence is accumulating that these mice are a useful animal model for investigating AD-like brain amyloidosis (senile plaque morphology) [4, 5, 14, 16, 28, 32]. In these mice, a 5-fold increase in Aβ_{1-40} and a 14-fold increase in A$\beta_{1-42/43}$ are found from 3 months to 9–10 months of age [14]. Moreover, Aβ deposits are associated with DNs, reactive microglia [9] and astroglia [16], resembling AD pathology [21]. Thus, the Tg2576 mice are considered to be good models of neuritic dystrophy caused by amyloid deposition [29]. However, unlike the case in AD, there are no NFTs, neuropil threads or overt neuronal loss in these mice [16].

Several other APP transgenic mouse models including PDAPP [12, 20], APP23 [33] and PSAPP [36] have been reported to demonstrate brain amyloidosis similar to that in Tg2576. Whereas age-dependent changes of amyloid deposition in such transgenic mice have been widely investigated, the formation of DNs has not been fully examined. In the present study, we investigated the immunohistochemical characteristics of phosphorylated-tau-positive DNs and carried out quantitative analysis of the DNs and congophilic plaques as a function of age in Tg2576 mice brains to clarify the mechanism of DNs formation.

Materials and methods

Animals

Female transgenic (tg) mice overexpressing human βAPP with the Swedish-type mutation, Tg2576 (HuAPP695, K670 N/M671L), were purchased from Taconic (NY, USA) and used in this experiment. They were given food and water ad libitum. Tg mice ranging in age from 11 to 20.5 months ($n=25$, 5 mice of 11 months, 3 mice of 12 months, 4 mice of 13 months, 3 mice of 17 months, 7 mice of 19 months and 3 mice of 20.5 months) were studied. Surgical and animal care procedures were carried out with strict adherence to the guidelines set forth in the National Institutes of Health Guide for the Care and Use of Laboratory Animals (publication 80-23). All attempts were made to minimize the number of animals used and their suffering.

Antibodies

The anti-phosphorylated-tau antibodies used in the present study were as follows. Monoclonal antibody AT8, which recognizes human tau phosphorylated at Ser202 and Thr205, was purchased from Innogenetics (BR-003, Gent, Belgium) [13]. Affinity-purified rabbit polyclonal antibody, which recognizes human tau phosphorylated at Ser396 was produced in house. Two rabbit polyclonal antibodies, R163 and R165, which are specific for the carboxy-terminal epitopes of Aβ_{1-40} and Aβ_{1-42}, respectively (diluted 1:300, affinity-purified rabbit IgG, provided by Dr. Mehta, IBR, NY) [23, 24] were used.

Tissue preparation

Each animal was perfused, under pentobarbital anesthesia (50 mg/kg, intraperitoneal injection), via the ascending aorta with 10 mM phosphate-buffered saline (PBS, pH 7.4), followed by a fixative containing 4% paraformaldehyde in 100 mM phosphate buffer (pH 7.4). After perfusion, the brain was quickly removed and immersed in the same fixative for 2 days, and then placed in 100 mM phosphate buffer (pH 7.4) containing 16% sucrose for 2 days. The brain was frozen with dry-ice and sagittally cut into 20-μm-thick sections with a cryostat (HM500-OM, Zeiss, Germany). The sections were collected in 100 mM PBS containing 0.3% Triton X-100 (PBST), and washed three times. All of the above procedures were conducted at 4°C.

Immunohistochemistry and Congo red staining

Immunohistochemical staining was carried out on free-floating sections. Sections were incubated for 3 days at 4°C with the primary antibodies listed above. The antibodies were detected using the Vectastain ABC (avidin-biotin-peroxidase complex) Elite kit (Vector Laboratories, CA). Labeling was visualized by incubating sections for 15 min with 50 mM Tris-HCl buffer (pH 7.6), containing 0.01% 3,3'-diaminobenzidine (Sigma Chemical Co, MO), 0.6% nickel ammonium sulfate, 0.1 M imidazole and 0.003% hydrogen peroxide. For double immunostaining, sections were co-incubated with antibodies AT8 and R163, or AT8 and R165, for 16 h at room temperature. The antibodies were detected using biotinylated anti-rabbit IgG/avidin-Texas Red and fluorescein isothiocyanate-labeled anti-mouse IgG antibody (Vector Laboratories). Fluorescence was observed

using a laser scanning microscope (Olympus, Tokyo, Japan). All immunoreagents were diluted with 100 mM PBST (pH 7.4), and sections were rinsed in 100 mM PBST (pH 7.4) after each step. The preferred dilution of the Ser396 antibody and AT8 were 1 μg/ml and 0.5 μg/ml, respectively, for the ABC detection system. For the fluorescence detection method, AT8 was used at a concentration of 1.5 μg/ml. For Aβ immunohistochemistry, sections were incubated with 100% formic acid for 1 min at room temperature before the primary antibody was applied.

Congo red staining [3, 34] was performed according to previously described methods [38]. In brief, after immunostaining, the brain section was mounted on a glass slide and air-dried, the section was pre-immersed in 80% ethanol containing 4% sodium chloride for 1 h, followed by immersion in 80% ethanol containing 0.2% Congo red for 1 h at room temperature. The sections were coverslipped and observed under a microscope with a reflex filter.

Digitalized quantification

Immunoreactive components in the brain sections were observed using an Olympus microscope equipped with a digital camera (Fujix digital camera HC-2500 3CCD, Fujifilm, Tokyo, Japan). The color image of congophilic plaques was obtained and trimmed individually. Image processing was performed following steps designed to reveal specifically labeled AT8-positive DNs or Congo red-positive plaques using Adobe Photoshop 5.0 (Adobe system Inc., CA). For extraction of DN structures, to eliminate Congo red staining (Red), the original color image was manipulated using color extraction steps (the red of RGB channel, the bright of picture mode). For whole plaque detection, to combine DNs with congophilic plaque, the original color image was manipulated using color extraction steps (the green of RGB channel, the dark of picture mode). The automatically converted gray scale images were analyzed for quantification of the DNs and plaque area with a Macintosh G3 computer using NIH image 1.6.1 program (developed at the US national Institutes of Health) (Fig. 1).

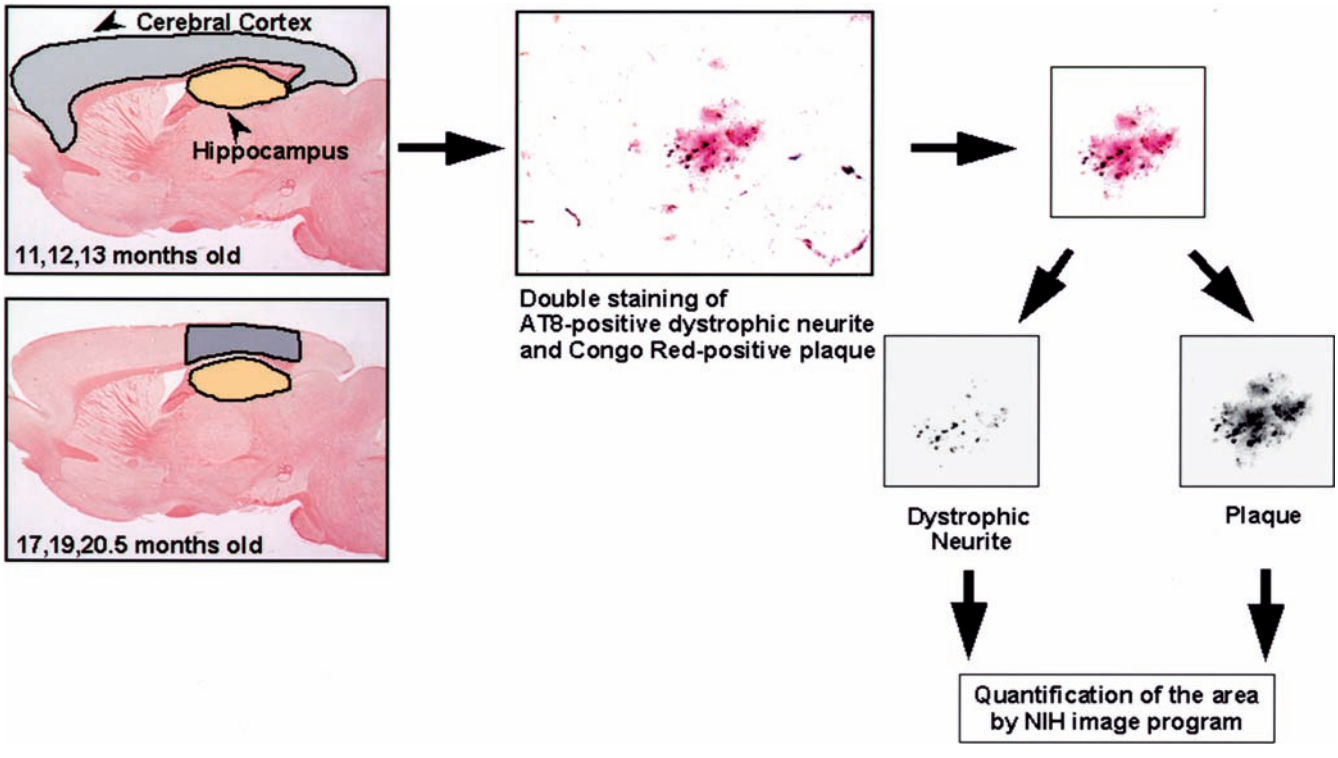

Fig. 1 Process of quantitative image analysis. Double staining of AT8-positive DNs (*black dotty structures* associated with congophilic plaque) and Congo red-positive plaques (*red structures*) were performed using sagittal sections of Tg2576 mice. The color image of each plaque was obtained individually by a microscope equipped with a digital camera, and was trimmed. For extraction of DN or plaque structures, the original color image was manipulated using a color extraction method (see Materials and Methods for details). The automatically converted gray scale images were analyzed for quantification of the DNs and area using NIH image program (*DNs* dystrophic neurites)

Measurement of AT8-positive dystrophic neurite and Congo red-positive plaque

The AT8-positive area and Congo red-positive area were separately quantified in each plaque. We analyzed 61 plaques at 11–13 months, 283 plaques at 17–19 months and 279 plaques at 20.5 months in the cerebral cortex, and 27 plaques at 11–13 months, 228 plaques at 17–

19 months and 191 plaques at 20.5 months in hippocampus. The sections were taken from five different levels (500-μm intervals extending laterally from 2.3 to 4.3 mm lateral to the midline). The AT8-positive DN areas and Congo red-positive plaque areas were calculated as the percentage of the cerebral cortical or hippocampal area in each section, and the average of the percentages at five parasagittal levels was used as an estimate of overall AT8-positive DN area and Congo red-positive plaque area in each animal at each age. Congophilic plaques in subfields of the cerebral cortex were examined in the case of older mice at the age of 17, 19 and 20.5 months (Fig. 1). The ratio of the AT8-positive DN area to the Congo red-positive plaque area of each plaque was calculated.

Results

Aberrant neurites were detected with anti-phosphorylated-tau antibodies, AT8 (tau phosphorylated at Ser202 and Thr205) and Ser396 (tau phosphorylated at Ser 396), throughout the cerebral cortex and hippocampus in Tg2576 mice at the age of 20.5 months. These structures were not found in wild-type mice at the same age (data not shown). The phosphorylated tau-immunoreactive aberrant structures were exclusively associated with congophilic plaques (Fig. 2A, B), and were reported to be accorded with DNs [39]. Only a few congophilic plaques in the cerebral cortex and hippocampus were associated with AT8-positive DNs

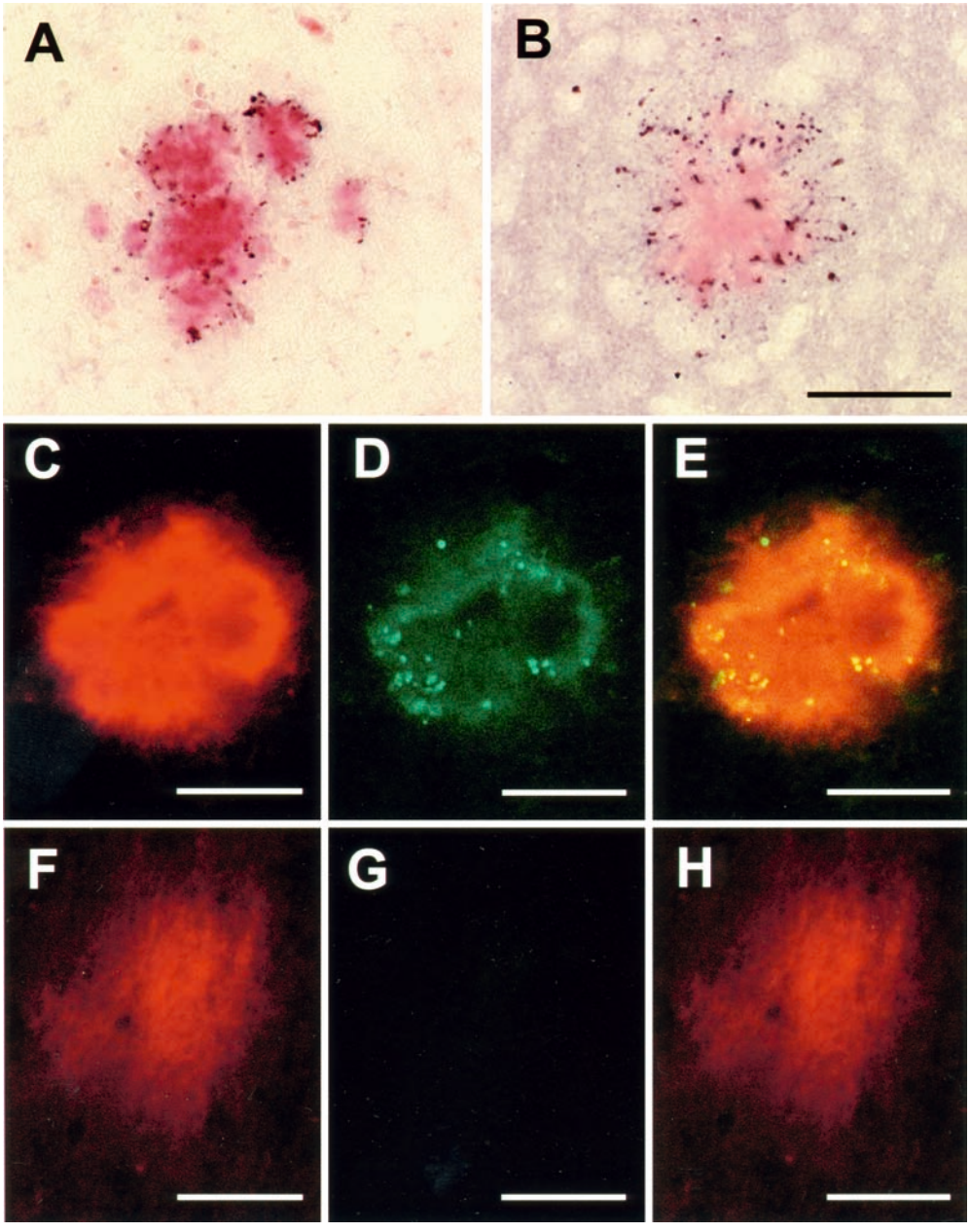

Fig. 2 Representative DNs, detected with anti-phosphorylated-tau antibodies, are exclusively associated with congophilic plaques in Tg2576 mice at the age of 20.5 months. DNs, which are immunopositive for the AT8 antibody (**A**) and the Ser 396 antibody (**B**), are colocalized with congophilic plaques. Merged image (**E**) shows that AT8-positive DNs (**D**) are associated with Aβ_{1-40}-positive (R163) plaques (**C**), while none of AT8-positive DNs (**G**) are associated with Aβ_{1-40}-negative/Aβ_{1-42}-positive (R165) plaques (**F**, **H**). *Bars* **A**, **B** 50 μm; **C**–**H** 30 μm

Table 1 The total number of Congo red-positive plaques examined, and the ratio of Congo red-positive plaques associated (+) or not (−) with AT8-positive DNs in the cerebral cortex and hippocampus in Tg2576 mice (*DNs* dystrophic neurites)

	Plaque number (% of total)		
	AT8-positive DN (+)	AT8-positive DN (−)	Total
Cerebral cortex	610 (97.9)	13 (2.1)	623 (100)
Hippocampus	440 (98.7)	6 (1.3)	446 (100)

(Table 1). Neither neuropil threads nor NFTs were detected with anti-phosphorylated-tau antibodies. To clarify the distribution of AT8-positive DNs within $A\beta_{1-40}$-positive and $A\beta_{1-42}$-positive plaques, respectively, double immunostaining was performed. Under a laser-confocal microscope, double immunostaining with AT8 (green, Fig. 2D) and with R163 for $A\beta_{1-40}$ (red, Fig. 2C) demonstrated that AT8-immunoreactive DNs associated with $A\beta_{1-40}$-positive plaque (merged images, yellow indicating co-localization of AT8-positive DNs and $A\beta_{1-40}$-positive plaques, Fig. 2E). Conversely, there were no AT8-immunoreactive DNs (green, Fig. 2G) associated with $A\beta_{1-42}$-positive plaques (Fig. 2F, G, H). No $A\beta_{1-42}$-positive plaque that had no AT8-positive DNs were immunostained for $A\beta_{1-40}$, nor were they stained with Congo red (data not shown). This observation showed AT8 to be the appropriate antibody for further quantitative analysis of DNs in Tg2576 mice, because AT8 showed a relatively low background staining compared to the Ser396 antibody.

Quantitative analyses of AT8-positive DNs and Congo red-positive plaques were performed in the cerebral cortex and hippocampus. Younger mice (11–13 months old) showed few Congo red-positive plaques, but the number increased with age and reached a notable figure at 17–19 months of age. At 20.5 months of age, Congo red-positive plaques were widely observed both in the cerebral cortex and hippocampus (Fig. 3A, B), resulting in a dramatic increase in congophilic plaque area (Fig. 3C, D). An increase in AT8-positive DN area accompanied the increase in Congo red-positive plaque number and plaque area (Fig. 3E, F). The area of Congo red-positive plaques increased 78-fold and 44-fold from 11–13 to 20.5 months of age in the cerebral cortex and

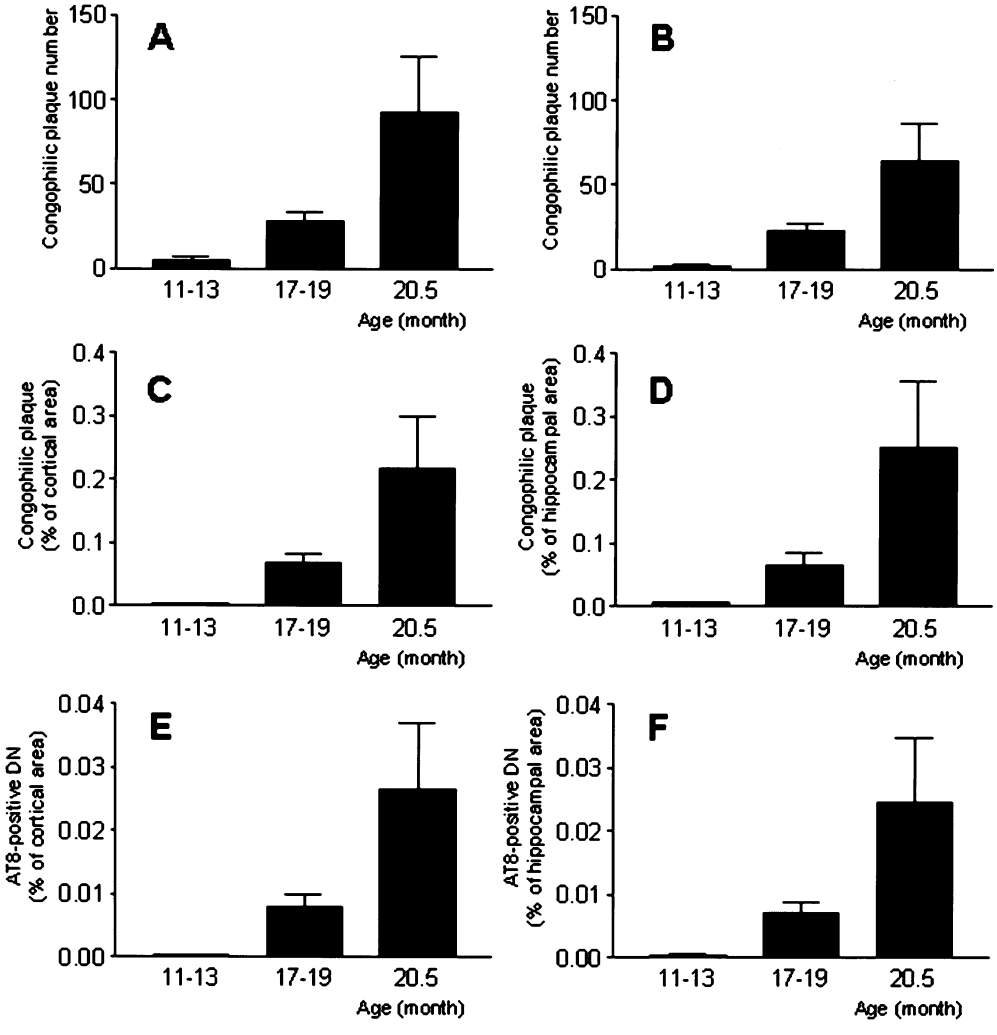

Fig. 3 The number of congophilic plaques (**A**, **B**), the congophilic plaque area (**C**, **D**) and the AT8-positive DN area (**E**, **F**) increase with age both in the cerebral cortex (**A**, **C**, **E**) and hippocampus (**B**, **D**, **F**). All data are expressed as mean + SE

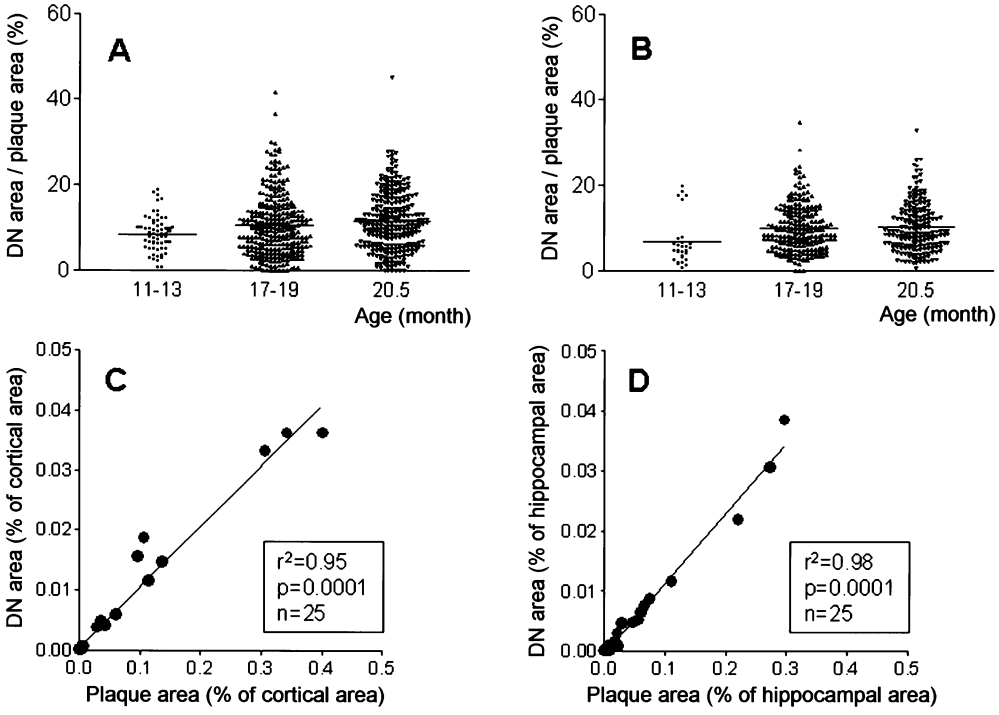

Fig. 4 The ratio of AT8-positive area to Congo red-positive area of each plaque at ages of 11–13, 17–19 and 20.5 months. The mean values of the ratio remain unchanged and are almost identical with age in both the cerebral cortex (**A**) and hippocampus (**B**). Total amount of AT8-positive DNs and congophilic plaques in each Tg2576 mouse (11–20.5 months, $n=25$) show significant positive correlation in the cerebral cortex (**C**) and hippocampus (**D**). Each plot indicates the total amount of AT8-positive DNs and congophilic plaques in five sagittal sections in a mouse

hippocampus, respectively. The area of AT8-positive DNs also increased 120-fold and 60-fold from 11–13 to 20.5 months of age in the cerebral cortex and hippocampus, respectively. The ratio of DN to Congo red area was quite similar at all ages examined (11–13, 17–19 and 20.5 months). The mean ratio was approximately 10%, and was unchanged with age in both the cerebral cortex and hippocampus (Fig. 4A, B). The plot of DN area versus plaque area for all the mice examined (11–20.5 months, $n=25$) showed significant positive correlations (cerebral cortex: $r^2=0.95$, $P=0.0001$; hippocampus: $r^2=0.98$, $P=0.0001$) (Fig. 4C, D). The average value for congophilic plaque areas did not change with age, and was equivalent in both the cerebral cortex and hippocampus (Fig. 5).

Discussion

In the present study, DNs in Tg2576 mice were clearly immunostained with anti-phosphorylated tau antibodies (AT8 and Ser396), and the DNs showed similar immunohistochemical and morphological characteristics to those in AD [27, 41]. We have also demonstrated that the aberrant neurites in Tg2576 mice are stained with synaptophysin and α-synuclein, and are associated with Congo red-positive plaques as in AD [38]. These data indicate that the plaque-associated DNs detected by phosphorylated tau antibodies have the same characteristics as those in AD. The AT8-positive DNs and Congo red-positive plaques were quantitatively analyzed in the present study. Quantitative data for DNs in AD brains have not been reported, because in AD brains NFTs and neuropil threads are also positive for phosphorylated tau. It may therefore be difficult to specifically identify DNs in the congophilic plaque. On the other hand, AT8-positive neuropil threads and NFTs were not found in Tg2576 mice in the present and previous experiments [29]. Taking these advantages into consideration, Tg2576 mice are a very useful model to investigate DNs and their mechanism of formation.

Notably, DNs positive for phosphorylated tau in Tg2576 mice were exclusively associated with congophilic plaques, and were not detected except in such the plaque association. Su et al. [35] reported that in aged

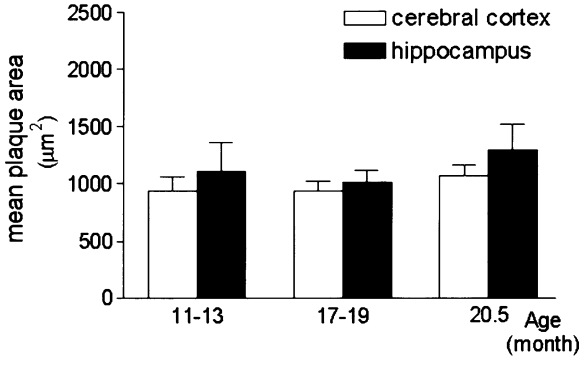

Fig. 5 The mean area of examined congophilic plaques is almost the same in mice from 11–13 to 20.5 months of age (61 plaques at 11–13 months, 283 plaques at 17–19 months and 279 plaques at 20.5 months in the cerebral cortex, and 27 plaques at 11–13 months, 228 plaques at 17–19 months and 191 plaques at 20.5 months in hippocampus), and is equivalent in both the cerebral cortex and hippocampus. All data are expressed as mean + SE

non-demented brain, approximately half of the plaques contained neurofilament (NF)-immunopositive DNs, but that PHF/tau-positive DNs were rarely detectable. In contrast, in the AD brain, 50% of the plaques contained PHF/tau-positive DNs. These data suggest that Congo red-positive plaques may be the most suitable marker for detecting amyloid plaques with DNs (neuritic plaques) associated with disease progression.

Neuritic plaques have been considered to be a pathological correlation of dementia in AD patients [26]. The present quantitative analysis showed dramatic increases in the number of congophilic plaques and in the area of DNs and Congo red-positive plaques in Tg2576 between 11 and 20.5 months of age. Westerman et al. [40] reported that age-dependent impairment in spatial reference memory occurred in Tg2576 mice. Therefore, age-dependent increase of congophilic plaques with AT8-positive DNs observed in this present study might reflect age-dependent memory deficits in Tg2576 mice.

It is interesting that despite the dramatic increase in DNs and plaque area with age in these animals, the mean ratio of DN area to congophilic plaque area was almost identical. These data suggest that the total amount of AT8-positive DNs and congophilic plaques are mainly responsible for the pathological progression, which elicits dementia, rather than the amount of DNs in each plaque. The synaptic deficits in Tg2576 mice might result from global disruptions in the neuronal network due to an increasing number of congophilic plaques and DNs, rather than from direct focal damage at individual sites by such plaques and DNs.

The mean area of congophilic plaque was unchanged with age in both the cerebral cortex and hippocampus (Fig. 5). A longitudinal in vivo imaging study in Tg2576 mice has shown that there is no detectable change in ThioS-positive plaque size over extended periods of time [6]. The effect of applying ThioS before imaging of plaques should be considered, because certain amyloid-binding molecules, such as Congo red, chrysamine G and ThioS can inhibit the formation of Aβ fibrils [18]. In this present study, congophilic plaques, like ThioS-positive plaques [6], existed as stable features (stable size and stable ratio of DNs to plaques) from early to late pathological stages in Tg2576 mice.

Although all congophilic plaques were associated with AT8-positive DNs, a few congophilic plaques did not have AT8-positive DNs (less than 2.5%), suggesting that the formation of congophilic plaques and AT8-positive DNs is simultaneous, or that the congophilic plaque formation may slightly precede DN formation. This prediction is consistent with a previous report concerning a grading system for pathological severity of AD, where appearance of Congo red-positive plaques precede that of neuritic plaques with tau-positive neurites [25].

We have previously demonstrated the following sequence of plaque formation: Aβ_{1-42} deposition precedes apoE deposition, while Aβ_{1-40} deposition, which is equivalent to congophilic plaque formation, follows apoE deposition [37]. Therefore Aβ_{1-40}-positive, congophilic plaques, which are associated with AT8-positive DNs, are amyloid plaques forming at a late stage in the pathological progression in Tg2576 mice. Iwatsubo et al. [17] have clearly shown that the initial Aβ deposition does not begin with Aβ_{1-40} but with Aβ_{1-42} or longer Aβ. Aβ_{1-42}-positive/Aβ_{1-40}-negative plaques may represent early-stage senile plaques. The proportion of Aβ_{1-40}-positive plaques increases during AD progression. The data are accordant with our present study, indicating pathology of amyloidosis in Tg2576 mice is similar to that of AD.

In conclusion, the present study showed that AT8-positive DNs are exclusively associated with congophilic plaques in Tg2576 mice, indicating the importance of congophilic plaques as a neuritic plaque marker. AT8-positive DNs and congophilic plaques increase dramatically with age. However, the quantitative relationship between AT8-positive DNs and Congo red-positive plaques is maintained with age, especially from the beginning of DN formation. These results suggest that the formation of DNs is closely associated with that of Congo red-positive plaques. The precise mechanisms of plaque formation should be examined in further studies.

References

1. Armstrong RA (1998) β-amyloid plaques: stages in life history or independent origin? Dement Geriatr Cogn Disord 9:227–238
2. Braak H, Braak E (1991) Neuropathological stageing of Alzheimer-related changes. Acta Neuropathol 82:239–259
3. Braak H, Braak E (1997) Staging of Alzheimer-related cortical destruction. Int Psychogeriatr 9:257–261
4. Carlson GA, Borchelt DR, Dake A, Turner S, Danielson V, Coffin JD, Eckman C, Meiners J, Nilsen SP, Younkin SG, Hsiao KK (1997) Genetic modification of the phenotypes produced by amyloid precursor protein overexpression in transgenic mice. Hum Mol Genet 6:1951–1959
5. Chapman PF, White GL, Jones MW, Cooper-Blacketer D, Marshall VJ, Irizarry M, Younkin L, Good MA, Bliss TV, Hyman BT, Younkin SG, Hsiao KK (1999) Impaired synaptic plasticity and learning in aged amyloid precursor protein transgenic mice. Nat Neurosci 2:271–276
6. Christie RH, Bacskai BJ, Zipfel WR, Williams RM, Kajdasz ST, Webb WW, Hyman BT (2001) Growth arrest of individual senile plaques in a model of Alzheimer's disease observed by in vivo multiphoton microscopy. J Neurosci 21:858–864
7. Dickson DW, Farlo J, Davies P, Crystal H, Fuld P, Yen SH (1988) Alzheimer's disease. A double-labeling immunohistochemical study of senile plaques. Am J Pathol 132:86–101
8. Fraser PE, Levesque L, McLachlan DR (1993) Biochemistry of Alzheimer's disease amyloid plaques. Clin Biochem 26:339–349
9. Frautschy SA, Yang F, Irrizarry M, Hyman B, Saido TC, Hsiao K, Cole GM (1998) Microglial response to amyloid plaques in APPsw transgenic mice. Am J Pathol 152:307–317
10. Fukumoto H, Asami-Odaka A, Suzuki N, Iwatsubo T (1996) Association of Aβ 40-positive senile plaques with microglial cells in the brains of patients with Alzheimer's disease and in non-demented aged individuals. Neurodegeneration 5:13–17
11. Fukumoto H, Asami-Odaka A, Suzuki N, Shimada H, Ihara Y, Iwatsubo T (1996) Amyloid β protein deposition in normal aging has the same characteristics as that in Alzheimer's disease. Predominance of Aβ 42(43) and association of Aβ 40 with cored plaques. Am J Pathol 148:259–265

12. Games D, Adams D, Alessandrini R, Barbour R, Berthelette P, Blackwell C, Carr T, Clemens J, Donaldson T, Gillespie F, et al (1995) Alzheimer-type neuropathology in transgenic mice overexpressing V717F β-amyloid precursor protein. Nature 373:523–527
13. Greenberg SG, Davies P (1990) A preparation of Alzheimer paired helical filaments that displays distinct tau proteins by polyacrylamide gel electrophoresis. Proc Natl Acad Sci USA 87:5827–5831
14. Hsiao K, Chapman P, Nilsen S, Eckman C, Harigaya Y, Younkin S, Yang F, Cole G (1996) Correlative memory deficits, Aβ elevation, and amyloid plaques in transgenic mice. Science 274:99–102
15. Ikeda K, Haga C, Kosaka K, Oyanagi S (1989) Senile plaque-like structures: observation of a probably unknown type of senile plaque by periodic-acid methenamine silver (PAM) electron microscopy. Acta Neuropathol 78:137–142
16. Irizarry MC, McNamara M, Fedorchak K, Hsiao K, Hyman BT (1997) APP_{Sw} transgenic mice develop age-related Aβ deposits and neuropil abnormalities, but no neuronal loss in CA1. J Neuropathol Exp Neurol 56:965–973
17. Iwatsubo T, Odaka A, Suzuki N, Mizusawa H, Nukina N, Ihara Y (1994) Visualization of Aβ 42(43) and Aβ 40 in senile plaques with end-specific Aβ monoclonals: evidence that an initially deposited species is Aβ 42(43). Neuron 13:45–53
18. Lorenzo A, Yankner BA (1994) β-amyloid neurotoxicity requires fibril formation and is inhibited by congo red. Proc Natl Acad Sci USA 91:12243–12247
19. Mann DM, Iwatsubo T, Ihara Y, Cairns NJ, Lantos PL, Bogdanovic N, Lannfelt L, Winblad B, Maat-Schieman ML, Rossor MN (1996) Predominant deposition of amyloid-β 42(43) in plaques in cases of Alzheimer's disease and hereditary cerebral hemorrhage associated with mutations in the amyloid precursor protein gene. Am J Pathol 148:1257–1266
20. Masliah E, Sisk A, Mallory M, Mucke L, Schenk D, Games D (1996) Comparison of neurodegenerative pathology in transgenic mice overexpressing V717F β-amyloid precursor protein and Alzheimer's disease. J Neurosci 16:5795–5811
21. McGeer PL, McGeer EG (1995) The inflammatory response system of brain: implications for therapy of Alzheimer and other neurodegenerative diseases. Brain Res Brain Res Rev 21:195–218
22. McKee AC, Kosik KS, Kowall NW (1991) Neuritic pathology and dementia in Alzheimer's disease. Ann Neurol 30:156–165
23. Mehta PD, Dalton AJ, Mehta SP, Kim KS, Wisniewski HM, Aisen PS (1997) Plasma amyloid β1–42 levels are increased in Down's syndrome but not in Alzheimer's disease. Ann Neurol 42 (Suppl M29):400
24. Mehta PD, Dalton AJ, Mehta SP, Kim KS, Sersen EA, Wisniewski HM (1998) Increased plasma amyloid β protein 1–42 levels in Down syndrome. Neurosci Lett 241:13–16
25. Metsaars WP, Hauw JJ, Welsem ME van, Duyckaerts C (2003) A grading system of Alzheimer disease lesions in neocortical areas. Neurobiol Aging 24:563–572
26. Mirra SS, Heyman A, McKeel D, Sumi SM, Crain BJ, Brownlee LM, Vogel FS, Hughes JP, Belle G van, Berg L (1991) The Consortium to Establish a Registry for Alzheimer's Disease (CERAD). Part II. Standardization of the neuropathologic assessment of Alzheimer's disease. Neurology 41:479–486
27. Onorato M, Mulvihill P, Connolly J, Galloway P, Whitehouse P, Perry G (1989) Alteration of neuritic cytoarchitecture in Alzheimer disease. Prog Clin Biol Res 317:781–789
28. Pappolla MA, Chyan YJ, Omar RA, Hsiao K, Perry G, Smith MA, Bozner P (1998) Evidence of oxidative stress and in vivo neurotoxicity of β-amyloid in a transgenic mouse model of Alzheimer's disease: a chronic oxidative paradigm for testing antioxidant therapies in vivo. Am J Pathol 152:871–877
29. Price DL, Tanzi RE, Borchelt DR, Sisodia SS (1998) Alzheimer's disease: genetic studies and transgenic models. Annu Rev Genet 32:461–493
30. Selkoe DJ (1994) Alzheimer's disease: a central role for amyloid. J Neuropathol Exp Neurol 53:438–447
31. Selkoe DJ (1998) The cell biology of β-amyloid precursor protein and presenilin in Alzheimer's disease. Trends Cell Biol 8:447–453
32. Smith MA, Hirai K, Hsiao K, Pappolla MA, Harris PL, Siedlak SL, Tabaton M, Perry G (1998) Amyloid-β deposition in Alzheimer transgenic mice is associated with oxidative stress. J Neurochem 70:2212–2215
33. Sturchler-Pierrat C, Abramowski D, Duke M, Wiederhold KH, Mistl C, Rothacher S, Ledermann B, Burki K, Frey P, Paganetti PA, Waridel C, Calhoun ME, Jucker M, Probst A, Staufenbiel M, Sommer B (1997) Two amyloid precursor protein transgenic mouse models with Alzheimer disease-like pathology. Proc Natl Acad Sci USA 94:13287–13292
34. Styren SD, Hamilton RL, Styren GC, Klunk WE (2000) X-34, a fluorescent derivative of Congo red: a novel histochemical stain for Alzheimer's disease pathology. J Histochem Cytochem 48:1223–1232
35. Su JH, Cummings BJ, Cotman CW (1998) Plaque biogenesis in brain aging and Alzheimer's disease. II. Progressive transformation and developmental sequence of dystrophic neurites. Acta Neuropathol 96:463–471
36. Takeuchi A, Irizarry MC, Duff K, Saido TC, Hsiao Ashe K, Hasegawa M, Mann DM, Hyman BT, Iwatsubo T (2000) Age-related amyloid β deposition in transgenic mice overexpressing both Alzheimer mutant presenilin 1 and amyloid β precursor protein Swedish mutant is not associated with global neuronal loss. Am J Pathol 157:331–339
37. Terai K, Iwai A, Kawabata S, Sasamata M, Miyata K, Yamaguchi T (2001) Apolipoprotein E deposition and astrogliosis are associated with maturation of β-amyloid plaques in βAPPswe transgenic mouse: implications for the pathogenesis of Alzheimer's disease. Brain Res 900:48–56
38. Terai K, Iwai A, Kawabata S, Tasaki Y, Watanabe T, Miyata K, Yamaguchi T (2001) β-amyloid deposits in transgenic mice expressing human β-amyloid precursor protein have the same characteristics as those in Alzheimer's disease. Neuroscience 104:299–310
39. Tomidokoro Y, Ishiguro K, Harigaya Y, Matsubara E, Ikeda M, Park JM, Yasutake K, Kawarabayashi T, Okamoto K, Shoji M (2001) Aβ amyloidosis induces the initial stage of tau accumulation in APP(Sw) mice. Neurosci Lett 299:169–172
40. Westerman MA, Cooper-Blacketer D, Mariash A, Kotilinek L, Kawarabayashi T, Younkin LH, Carlson GA, Younkin SG, Ashe KH (2002) The relationship between Aβ and memory in the Tg2576 mouse model of Alzheimer's disease. J Neurosci 22:1858–1867
41. Yilmazer-Hanke DM (1998) Pathogenesis of Alzheimer-related neuritic plaques: AT8 immunoreactive dystrophic neurites precede argyrophilic neurites in plaques of the entorhinal region, hippocampal formation, and amygdala. Clin Neuropathol 17:194–198